Journal of Power Sources 246 (2014) 840–845

Contents lists available at ScienceDirect

Journal of Power Sources

journal homepage: www.elsevier.com/locate/jpowsour

Short communication

Characterization of the solid electrolyte interphase on lithium anode for preventing the shuttle mechanism in lithium–sulfur batteries

Shizhao Xiong*, Kai Xie, Yan Diao, Xiaobin Hong

Department of Material Science and Engineering, College of Aerospace Science and Engineering, National University of Defense Technology, Changsha, Hunan 410073, PR China

HIGHLIGHTS

- Mechanism of the SEI for preventing the shuttle in Li–S batteries.
- $LiNO_3$ and polysulfides are equally important for preventing the shuttle.
- The SEI film for preventing the shuttle has multilayer structure.

ARTICLE INFO

Article history:
Received 30 April 2013
Received in revised form
10 July 2013
Accepted 16 August 2013
Available online 22 August 2013

Keywords:
Solid electrolyte interphase
Lithium nitrate
Polysulfides
Shuttle
Lithium–sulfur batteries

ABSTRACT

To understand the mechanism for preventing the shuttle in lithium–sulfur batteries, the SEI films formed in different electrolyte solutions are studied using X-ray photoelectron spectroscopy (XPS), scanning electron microscope (SEM) and electrochemical measurements. The SEI film formed in electrolyte solution with $LiNO_3$, which is an effective additive to suppress the shuttle, cannot maintain a stable state without polysulfides. The combination of electrochemical data and SEM images indicate that the contribution of $LiNO_3$ and polysulfides are equally important to form a SEI film which is effective in suppressing the shuttle. This SEI film can be assumed to consist of two sub layers, the top layer composed of oxidized products from polysulfides (lithium sulfates) and the bottom layer composed of the reduced products of polysulfides and $LiNO_3$ (lithium sulfide and LiN_xO_y). We suppose the formation process of this SEI film in detail and give a possible explanation of the mechanism by which the SEI film on the lithium electrode is preventing the shuttle in lithium–sulfur batteries.

1. Introduction

There is no doubt that the demand for clean and efficient energy storage devices is becoming more and more critical for future markets, such as plug-in hybrid vehicle and electric vehicle technologies [1,2]. Lithium battery system is one of the most promising candidates owing to their high specific energy and power density [1,3]. Nevertheless, the overall energy density of commercial lithium ion batteries is not enough to meet the demands of key applications [3,4]. In this regard, the lithium–sulfur batteries are receiving considerable interest at the present time, due to their high theoretical energy density (about 2600 Wh kg^{-1}), natural abundance of key elements and environmental friendliness [2,5,6]. However, the implementation of rechargeable lithium–sulfur batteries suffers from the capacity degradation upon cycling and low coulombic efficiency, which is mainly caused by high solubility of the polysulfides [2,7]. The polysulfides are formed as reaction intermediates throughout the discharge–charge process. Their migration results in loss of active material and a shuttle mechanism, which lead to the issues of lithium–sulfur batteries [8,9].

During the past decade, most attempts to overcome these issues have focused on the improving sulfur cathode to prevent the negative effects of the polysulfides, for example by using new materials for the carbon matrix [6,10–12] and modified active materials [5,13–15]. However, the lithium anode in lithium–sulfur batteries, which is directly involved in the active material loss and the shuttle mechanism, has not attracted enough attention [16]. The soluble polysulfides migrate through the separator and immediately react with the lithium anode, which lead to the active material loss [17,18]. Furthermore, the reaction products (reduced polysulfides) diffuse back to the sulfur cathode to generate the higher-order polysulfides again, creating a shuttle mechanism which leads to the low coulombic efficiency [19–21]. Hence, the behavior of the lithium anode plays a key role in overcoming the

* Corresponding author.
E-mail addresses: shizhao.xiong@hotmail.com, sxiong@nudt.edu.cn (S. Xiong).

0378-7753/$ – see front matter © 2013 Elsevier B.V. All rights reserved.
http://dx.doi.org/10.1016/j.jpowsour.2013.08.041

challenges of lithium–sulfur batteries. The consensus is that the behavior of lithium anode in nonaqueous electrolyte solution is controlled by the solid electrolyte interphase (SEI) which covers the active lithium metal [22]. The SEI film comes from the reaction between active lithium metal and the components of electrolyte solution, including organic solvents and anions of lithium salt [22,23]. Because of the soluble polysulfides, the properties of the SEI film on the lithium anode for lithium–sulfur batteries are different from the lithium electrodes reported before [16,24–26].

$LiNO_3$ has been found as an effective additive to prevent the detrimental shuttle in lithium–sulfur batteries [26], but the details about this effect have stayed unclear. In this paper, the SEI film on lithium anode cycling in different electrolyte solutions were characterized using X-ray photoelectron spectroscopy (XPS), scanning electron microscope (SEM) and electrochemical impedance spectroscopy (EIS) to understand this effect. Furthermore, the relationship between the shuttle and the SEI film is discussed in detail and the ideal SEI film for the lithium anode in lithium–sulfur batteries is introduced. As a strong oxidative agent, $LiNO_3$ in the electrolyte solution reduces the safety of lithium–sulfur batteries and results in irreversible active mass oxidation on the cathode [27]. With the discussion in this paper it should be possible for researchers to develop new additives for the improvement of lithium–sulfur batteries.

2. Experimental

The symmetrical coin cells were assembled to study the electrochemical performance of lithium electrodes in different electrolyte solutions. The electrolytes solution consisted of lithium salt (total concentration, 0.2 M) in 1,3-dioxolane (DIOX) and 1,2-dimethoxyethane (DME, 1:1, v/v) mixed solvents. Lithium metal foil (100 μm, Denway, China) was cut into 10 mm diameter disks as lithium electrodes. Each lithium disk was washed by dried hexane (water content < 20 ppm, Sigma–Aldrich) before assembling cells. A separator (Celgard® 2500, 20 μm thick) was added to separate

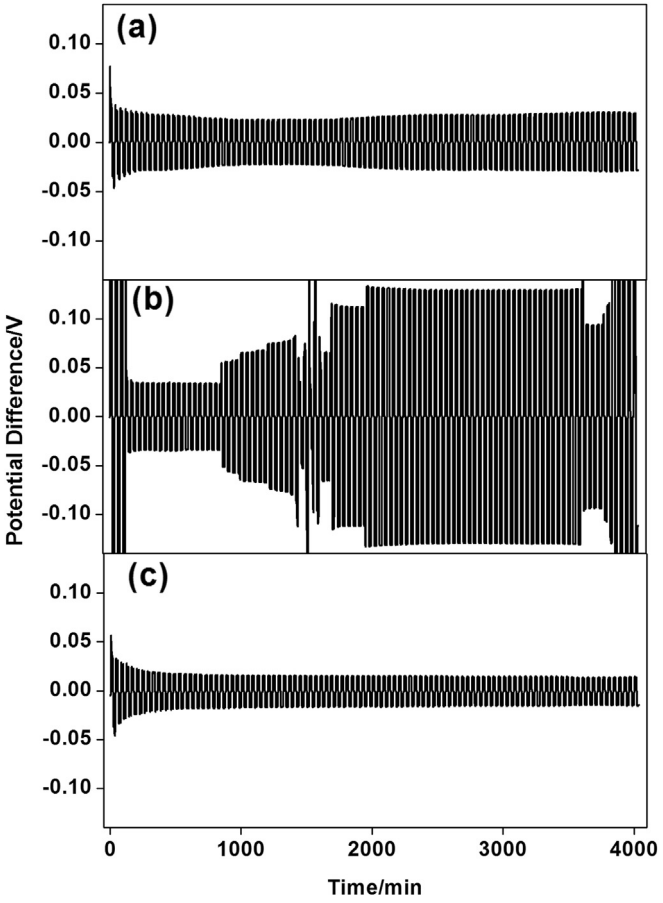

Fig. 1. Cycling behavior of a symmetrical cell with the electrolytes (a) 0.2 M Li_2S_6/DIOX/DME (1:1, v/v), (b) 0.2 M $LiNO_3$/DIOX/DME (1:1, v/v) and (c) 0.1 M $LiNO_3$/0.1 M Li_2S_6/DIOX/DME (1:1, v/v).

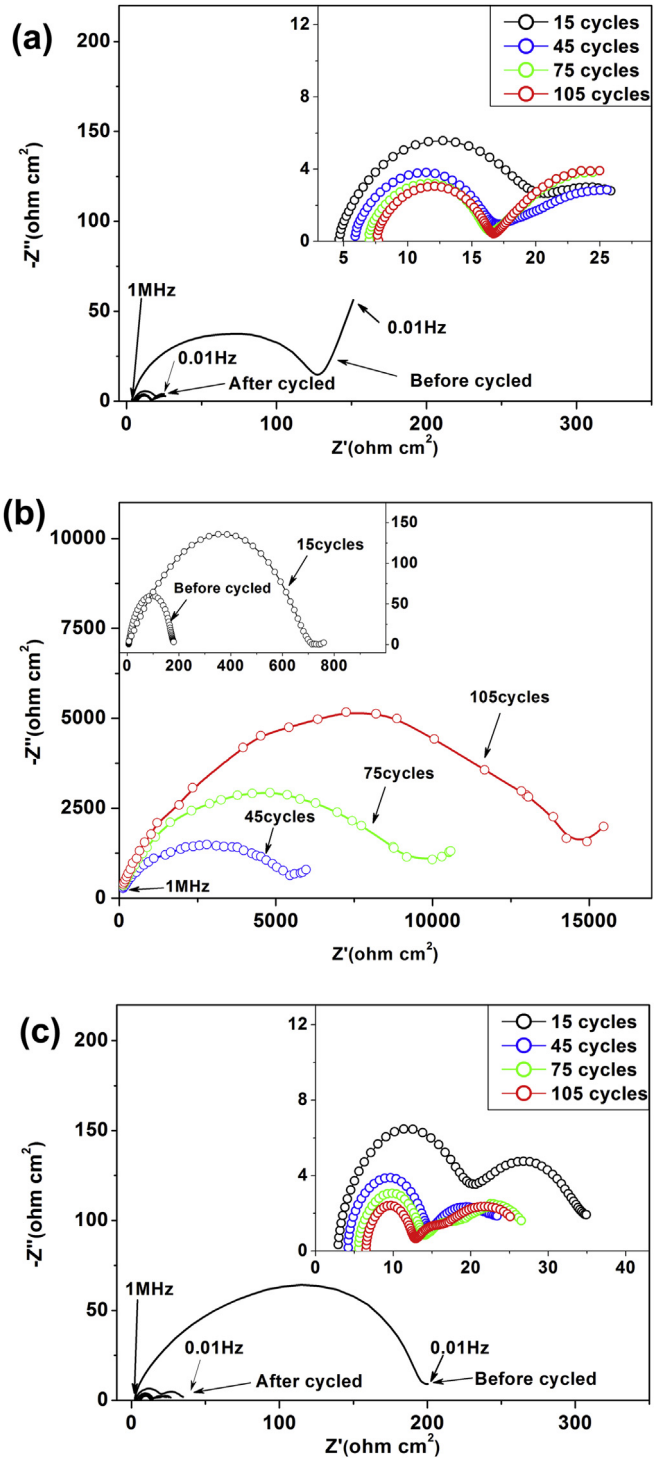

Fig. 2. Impedance spectra from the symmetrical cells containing (a) 0.2 M Li_2S_6/DIOX/DME (1:1, v/v), (b) 0.2 M $LiNO_3$/DIOX/DME (1:1, v/v) and (c) 0.1 M $LiNO_3$/0.1 M Li_2S_6/DIOX/DME (1:1, v/v).

the two Li electrodes. The cycling performance of the symmetrical cells was tested using a multi-channel battery test system (LAND CT2001A) at a current density of 0.40 mA cm^{-2}, each cycle consisting of 15 min charge, 15 min discharge and 5 min open circuit between them.

Lithium and sulfur (99.98%, Aldrich) in stoichiometric ratio were added into mixed solvents mentioned previously to prepare Li_2S_6 solution. The mixture was stirred vigorously for 24 h at 50 °C for the complete reaction of lithium with sulfur. All the operations were conducted in a glove-box full of argon.

The cycled cells were disassembled to retrieve the lithium electrodes for further characterization. All lithium electrodes were rinsed using 1,2-dimethoxyethane and further dried in a glove-box for 2 h. An Autolab Electrochemical Workstation (AUT71864) was operated to get impedance spectroscopy, using over a frequency range of 0.01 Hz to 1 MHz with perturbation amplitude was 5 mV.

A special transfer system described previously [25] was used to transferred lithium samples from the glove box to the SEM system (HTACHI S-4800) or the XPS systems (K-Alpha 1063, Thermo Fisher Scientific) without exposing them to atmosphere. An Al-Kα radiation (72 W, 12 kV) at a pressure of 10^{-9} Torr was used to obtain the X-ray photoelectron spectra. The diameter of the analyzed area was 400 μm. An argon ion beam (accelerating voltage 2 keV, ion beam current 6 μA) was employed to perform the etching process.

3. Results and discussion

Lithium metal is the only electrode material present in lithium symmetrical cells. Hence, the changes of the potential difference under a constant current indicate the stability and resistance of the system over cycles [28]. The curves of the symmetrical cell cycled with polysulfides (Fig. 1(a)) show that the potential difference decreases slightly to a stable one at the beginning of cycling. The increasing potential difference after 2000 min indicates that the SEI film on the lithium electrode changes slowly over cycles. Compared to other cells, the cell cycled in the electrolyte solution with $LiNO_3$ (Fig. 1(b)) as the lithium salt shows a much higher potential difference during the cycling. Furthermore, the curves show an irregular potential difference in spite of some stable periods. It suggests that the properties of this SEI film dramatically changes (such as broken) during cycling and it has a higher resistance for the transfer of Li-ion. This change indicates that it is repeatedly broken during cycling. At the same time, the broken SEI film can be repaired by the reaction between lithium electrode and the component of the electrolyte solution [16]. This results in the periods of relatively stable potential difference during the cycling and an increasing thickness of the SEI film. Considering the actual charge–discharge process of lithium–sulfur batteries, both soluble polysulfides and $LiNO_3$ were added into electrolyte solution for a symmetrical cell. As shown in Fig. 1(c), the potential difference of the cell maintains a stable leveling after the slight deceasing at the first few cycles. We suppose that the potential difference decrease at the beginning of cycling in Fig. 1(a) and (c) can be attributed to the breaking of the native surface film on the lithium electrode and the rebuilding of the SEI film. However, the presence of polysulfides seems to prevent the continuous reaction and maintains a stable SEI film on the lithium electrode.

Electrochemical impedance spectra (EIS) were employed to further understand the behavior of the SEI films formed in different electrolyte solutions. As shown in Fig. 2, the transfer of Li-ion across

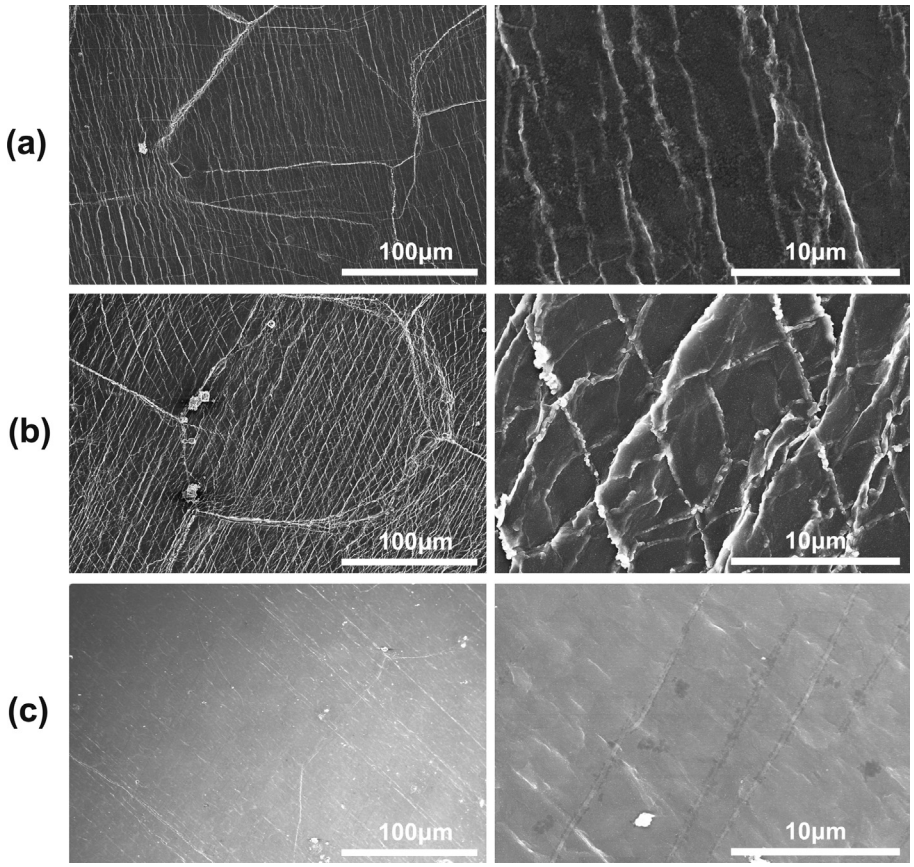

Fig. 3. SEM images of lithium electrodes cycling for 20 times in (a) 0.2 M Li_2S_6/DIOX/DME (1:1, v/v), (b) 0.2 M $LiNO_3$/DIOX/DME (1:1, v/v) and (c) 0.1 M $LiNO_3$/0.1 M Li_2S_6/DIOX/DME (1:1, v/v). Left column: low magnification, right column: high magnification.

Table 1
Summary of XPS data and assignments for SEI film on lithium electrode cycling in 0.1 M $LiNO_3$/0.1 M Li_2S_6/DIOX/DME (1:1, v/v) for 20 times.

Element	Peak position/eV	Assignment
Li 1s	53.1	Li
	53.7	Li_2O
	54.8	$ROCO_2Li$
	55.9	LiN_xO_y
C 1s	284.7	RCH_2OLi
	285.8	CH_3OCO_2Li
	288.4	CH_3CO_2Li
	289.8	Li_2CO_3
N 1s	394.6	RCH_2NO_2
	396.7	N–O (LiN_xO_y)
	399.1	Li_3N
	400.9	$Li_2N_2O_2$
O 1s	528.2	Li_2O
	529.0	ROLi
	531.0	Li_2CO_3
	531.7	S–O (Li_2SO_4, $Li_2S_2O_3$)
S 2p	160.8	Lithium sulfide
	162.1	Lithium sulfide
	164.3	$Li_2S_2O_3$
	168.3	Li_2SO4

the surface film contributes the main part of the resistance for the lithium electrodes before cycling [29,30]. The resistance of the lithium electrode immersed in electrolyte solution with polysulfides is lower than that with $LiNO_3$. It suggests that the SEI film formed with polysulfides gets a higher conductivity for the transfer of Li-ion. During the cycling, the spectra of the cell cycling with $LiNO_3$ (Fig. 2 (b)) only show one semicircle for the transfer of Li-ion in the SEI film. The dramatically increasing resistance indicates a continuous decomposition reaction of the electrolyte solution on the lithium electrode and a growing thickness of the SEI film. However, the spectra of the cells cycling with polysulfides (Fig. 2(a) and (c)) show two semicircles, corresponding to the Li-ion migration though the SEI film (high frequency semicircle) and the charge transfer across the interface (low frequency semicircle) respectively [31,32]. It suggests that the presence of polysulfides in electrolyte solution results in a different structure of the SEI film which has an obvious resistance for the charge transfer from the SEI film to lithium metal. Furthermore, the cells cycled with polysulfides show significantly decreased impedance for the Li-ion transfer through the SEI film at the beginning of cycling, even with the presence of $LiNO_3$. After 45 cycles, they show stable impedance with increasing cycles. This indicates that the presence of polysulfides in the electrolyte solution also results in a stable conductivity of the SEI film during cycling. Additionally, it confirms that the potential reaction between the lithium electrode and the electrolyte solution with $LiNO_3$ can be prevent by the SEI film formed with polysulfides.

To understand the behavior of SEI film on the lithium electrodes cycling in different electrolyte solutions, scanning electron microscopy was employed to obtain the morphology of the cycled lithium electrodes. As shown in Fig. 3(a), the SEI film on the lithium electrode cycling with polysulfides shows a rough morphology although it maintained a stable impedance and potential change in previous electrochemical measurements. It suggests that the reaction between polysulfides and lithium electrodes contributes to the formation of the surface film. The reaction products (lithium sulfide [16]) depositing on the lithium electrode can react with polysulfides and dissolve in the electrolyte solution once more [21]. Finally, the reaction comes to a balance after a continuous deposition–dissolution process. We suppose that the banded morphology of the SEI film can be attributed to the repeating deposition–dissolution process. Substantial debris can be seen on the surface of the lithium electrode cycling with $LiNO_3$ as lithium salt for 20 times (Fig. 3(b)). Combined with the previous results, it suggests that the reaction between lithium electrodes and electrolyte solution with $LiNO_3$ is active during the entire cycling. Furthermore, the ongoing deposition of the reaction products leads to the increasing resistance for the transfer of Li-ion across the SEI film. However, the lithium electrode cycling in the electrolyte solution with mixed lithium salts ($LiNO_3$ and lithium

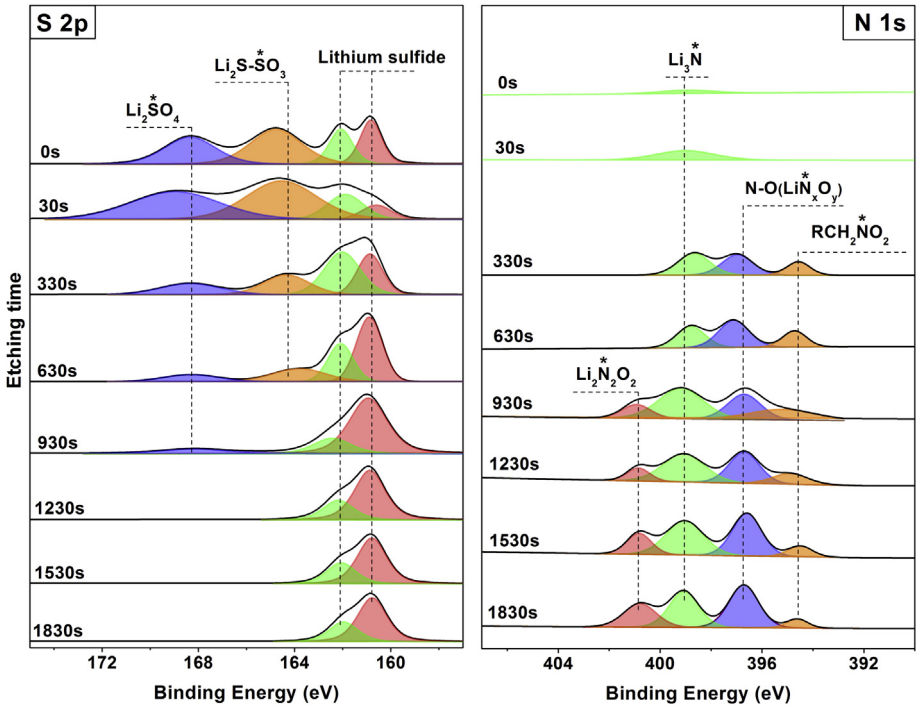

Fig. 4. X-ray photoelectron spectroscopy (XPS) spectra from a lithium electrode cycling in 0.1 M $LiNO_3$/0.1 M Li_2S_6/DIOX/DME (1:1, v/v) for 20 times.

polysulfides) shows a relatively smooth morphology with a little amount of deposition. This indicates that the deposition of both lithium polysulfides and $LiNO_3$ have been suppressed by the unique SEI film formed in the electrolyte solution with the two lithium salts.

In order to understand the structure of the SEI film formed in the electrolyte solution with mixed lithium salts ($LiNO_3$ and lithium polysulfides), X-ray photoelectron spectroscopy (XPS) and argon-ion sputtering technology were employed to obtain the chemical composition and depth profile information of the film. As shown in Table 1, these peaks show the complicated reaction between the lithium metal and the components of the electrolyte solution. The decomposition products of the solvents (RCH_2OLi, ROLi) [16] and the reduced products of $LiNO_3$ (LiN_xO_y, $Li_2N_2O_2$) [16,25] are shown in the SEI film. For the S2p spectra, lithium sulfide can be attributed to the reduced products of the polysulfides in the electrolyte solution [16]. Compounds with S–O (Li_2SO_4, $Li_2S_2O_3$) [16,27] and–CO_2Li (CH_3CO_2Li, CH_3OCO_2Li) [33] indicate that $LiNO_3$ plays an important role as oxidizing agent in the formation of the SEI film.

Turning to the depth profile, the S 2p spectra in Fig. 4 shows that most of the oxidized products from polysulfides (Li_2SO_4, $Li_2S_2O_3$) deposit in the top layer of the SEI film. Under the top layer, most of sulfur element comes from lithium sulfide which is the reduced products of the polysulfides. However, for the N 1s spectra most of the reduced products from $LiNO_3$ ($Li_2N_2O_2$, LiN_xO_y) deposit in the bottom layer of the SEI film. This distribution of chemical composition is demonstrated by the depth profiles of each element in the surface film formed with mixed lithium salts, as shown in Fig. 5(a). The S concentration is considerably higher in the top layer, decreasing with the increasing depth to a constant level in the bottom layer. However, the N concentration is rarely detected in the top layer and increases to a constant level which is similar to the level of S concentration in the bottom layer. Obviously, the SEI film on the lithium electrode cycling in the electrolyte solution with mixed lithium salts ($LiNO_3$ and Li_2S_6) can be divided to two sub layers. The top layer is mainly composed of the oxidized products from polysulfides and the bottom layer is mainly composed of reduced products of polysulfides and $LiNO_3$. The SEI film with this unique structure can prevent the shuttle phenomenon in lithium–sulfur batteries and maintain a stable interphase during cycling. However, the depth profiles of the surface films formed with $LiNO_3$ and Li_2S_6 respectively show a decreasing concentration of N and S from the top layer to the bottom layer, as shown in Fig. 5(b) and (c).

On the basis of the data above we suppose the formation process of this SEI film on the lithium electrode shown in Fig. 6. Because of the strong oxidation of $LiNO_3$, the SEI film formed in the electrolyte solution with $LiNO_3$ keeps growing during cycling. This results in an increasing thickness of the film and substantial debris on the lithium electrode. For the lithium electrode cycling in the electrolyte solution with lithium polysulfides as lithium salt, the repeating deposition–dissolution reaction between polysulfides and lithium sulfide results in a relatively stable SEI film. However, this formation process is much more complicated on the lithium electrode cycling in the electrolyte solution with mixed lithium salts ($LiNO_3$ and lithium polysulfides). At the beginning of cycling, the reduced products of $LiNO_3$ and polysulfides deposit on the lithium electrode at the same time. As shown in the SEM images in Fig. 3, the co-precipitation of the products results in a smooth and compact layer by which the continuous reaction between lithium salts and lithium metal are prevented. This assumption can be indicated by the behavior of over potential and impedance in Figs. 1 and 2. After that, the polysulfides in electrolyte solution are oxidized to lithium sulfates by $LiNO_3$ and deposit above the previous layer, as indicated in Figs. 4 and 5. The top layer blocks the contact between the polysulfides in electrolyte solution and reductive species on lithium electrode, such as lithium metal and lithium sulfide. Thus, the shuttle phenomenon in lithium–sulfur batteries with $LiNO_3$ as lithium salt or additive is prevented in this way. We suggest that the SEI film with this structure could be the ideal one for the lithium anode in lithium–sulfur batteries.

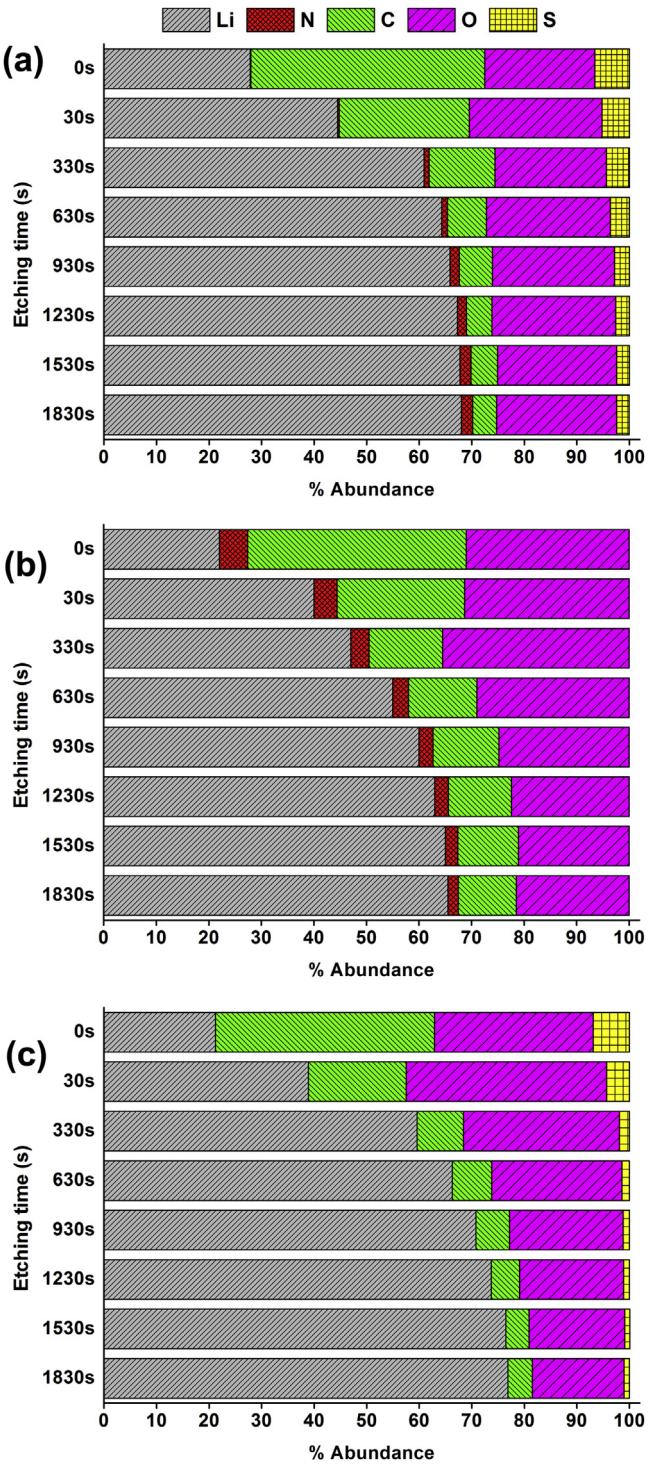

Fig. 5. Depth profile for the lithium anode surface cycling in (a) 0.1 M $LiNO_3$/0.1 M Li_2S_6/DIOX/DME (1:1, v/v), (b) 0.2 M $LiNO_3$/DIOX/DME (1:1, v/v) and (c) 0.2 M Li_2S_6/DIOX/DME (1:1, v/v) for 20 times.

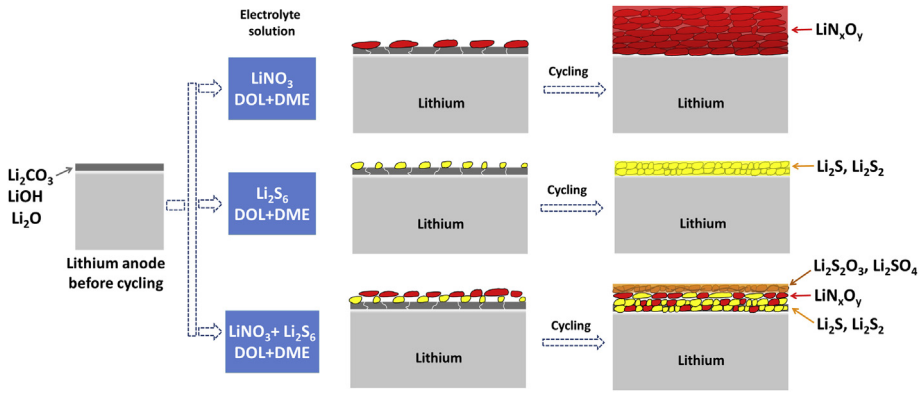

Fig. 6. Illustration of the surface film behavior on lithium anode cycling in different electrolyte solutions.

4. Conclusions

To understand the role of the SEI film in preventing the detrimental shuttle mechanism in lithium–sulfur batteries, the behavior of the SEI films on lithium electrodes cycling in different solutions was investigated using electrochemical measurements and scanning electron microscope images. Those results indicate that the SEI film formed in the electrolyte solution with mixed lithium salts ($LiNO_3$ and lithium polysulfides) is relatively stable during cycling. The unique structure of this SEI film was characterized by X-ray photoelectron spectroscopy and argon-ion sputtering technology. This SEI film can be assumed to be formed of two sub layers with the top layer composed of oxidized products from polysulfides and the bottom layer composed of the reduced products of polysulfides and $LiNO_3$. We suppose that the co-precipitation of the reduced products from $LiNO_3$ and lithium polysulfides results in a smooth and compact layer by which the continuous reaction on the lithium electrode is suppressed. Furthermore, the subsequent deposition of lithium sulfates results in a top layer consisting of relatively stable compounds. This top layer plays a significant role to prevent the contact between the polysulfides in electrolyte solution and reductive species on lithium electrode. Thus, the shuttle mechanism can be suppressed in the lithium–sulfur batteries with $LiNO_3$ as lithium salt or additive. The results and discussion in this paper will be helpful for researchers to develop new additive for the improvement of lithium–sulfur batteries.

Acknowledgments

We are grateful to the support of aid program for Science and Technology Innovative Research Team in Higher Educational Institutions of Hunan Province. The authors thank Erik Blomberg for his valuable discussions and input to the work.

References

[1] M. Armand, J.M. Tarascon, Nature 451 (2008) 652–658.
[2] P.G. Bruce, S.A. Freunberger, L.J. Hardwick, J.M. Tarascon, Nat. Mater. 11 (2012) 19–29.
[3] N.S. Choi, Z. Chen, S.A. Freunberger, X. Ji, Y.K. Sun, K. Amine, G. Yushin, L.F. Nazar, J. Cho, P.G. Bruce, Angew. Chem. Int. Ed. 51 (2012) 9994–10024.
[4] B. Scrosati, J. Garche, J. Power Sources 195 (2010) 2419–2430.
[5] Y. Yang, M.T. McDowell, A. Jackson, J.J. Cha, S.S. Hong, Y. Cui, Nano Lett. 10 (2010) 1486–1491.
[6] X. Ji, K.T. Lee, L.F. Nazar, Nat. Mater. 2460 (2009) 500–506.
[7] V.S. Kolosnitsyn, E.V. Karaseva, Russ. J. Electrochem 44 (2006) 548–552.
[8] S.E. Cheon, K.S. Ko, J.H. Cho, S.W. Kim, E.Y. Chin, J. Electrochem. Soc. 150 (2003) A796–A799.
[9] S.E. Cheon, K.S. Ko, J.H. Cho, S.W. Kim, E.Y. Chin, J. Electrochem. Soc. 150 (2003) A800–A805.
[10] B. Zhang, X. Qin, G.R. Li, X.P. Gao, Energy Environ. Sci. 3 (2010) 1531–1537.
[11] L. Ji, M. Rao, H. Zheng, L. Zhang, Y. Li, W. Duan, J. Guo, E.J. Cairns, Y. Zhang, J. Am. Chem. Soc. 133 (2011) 18522–18525.
[12] H. Wang, Y. Yang, Y. Liang, J.T. Robinson, Y. Li, A. Jackson, Y. Cui, H. Dai, Nano Lett. 11 (2011) 2644–2647.
[13] Y. Yang, G. Zheng, S. Misra, J. Nelson, M.F. Toney, Y. Cui, J. Am. Chem. Soc. 134 (2012) 15387–15394.
[14] K. Cai, M.K. Song, E.J. Cairns, Y. Zhang, Nano Lett. 12 (2012) 6474–6479.
[15] S. Xin, L. Gu, N.H. Zhao, Y.X. Yin, L.J. Zhou, Y.G. Guo, L.J. Wan, J. Am. Chem. Soc. 134 (2012) 18510–18513.
[16] D. Aurbach, E. Pollak, R. Elazari, G. Salitra, C.S. Kelley, J. Affinito, J. Electrochem. Soc. 156 (2009) A694–A702.
[17] K. Kumaresan, Y.V. Mikhaylik, R.E. White, J. Electrochem. Soc. 155 (2008) A576–A582.
[18] H.S. Ryu, Z. Guo, H.J. Ahn, G.B. Cho, H. Liu, J. Power Sources 189 (2009) 1179–1183.
[19] S.E. Cheon, S.S. Choi, J.S. Han, Y.S. Choi, B.H. Jung, H.S. Lima, J. Electrochem. Soc. 151 (2004) A2067–A2073.
[20] Y.V. Mikhaylik, J.R. Akridge, J. Electrochem. Soc. 150 (2003) A306–A311.
[21] Y.V. Mikhaylik, J.R. Akridge, J. Electrochem. Soc. 151 (2004) A1969–A1976.
[22] E. Peled, J. Electrochem. Soc. 126 (1979) 2047–2051.
[23] E. Peled, D. Golodnitsky, G. Ardel, J. Electrochem. Soc. 144 (1997) L208–L210.
[24] S. Xiong, K. Xie, Y. Diao, X. Hong, J. Power Sources 236 (2013) 181–187.
[25] S. Xiong, K. Xie, Y. Diao, X. Hong, Electrochim. Acta 83 (2012) 78–86.
[26] X. Liang, Z. Wen, Y. Liu, M. Wu, J. Jin, H. Zhang, X. Wu, J. Power Sources 196 (2011) 9839–9843.
[27] Y. Diao, K. Xie, S. Xiong, X. Hong, J. Electrochem. Soc. 159 (2012) A1816–A1821.
[28] G.H. Lane, A.S. Best, D.R. MacFarlane, M. Forsyth, A.F. Hollenkamp, Electrochim. Acta 55 (2010) 2210–2215.
[29] M.A. Vorotyntsev, M.D. Levi, A. Schechter, D. Aurbach, J. Phys. Chem. B 105 (2001) 188–194.
[30] A. Zaban, E. Zinigrad, D. Aurbach, J. Phys. Chem. 100 (1996) 3089–3101.
[31] J.G. Thevenin, R.H. Muller, J. Electrochem. Soc. 134 (1987) 273–280.
[32] D. Aurbach, K. Gamolsky, B. Markovsky, Y. Gofer, M. Schmidt, U. Heider, Electrochim. Acta 47 (2002) 1423–1439.
[33] L.J. Rendek, G.S. Chottiner, D.A. Scherson, J. Electrochem. Soc. 149 (2002) E408–E412.